Design of austenitic and duplex stainless steel SHS and RHS beam-columns

Design of austenitic and duplex stainless steel SHS and RHS beam-columns

Ju Chen[1], Yuner Huang[2,*], Ben Young[3]

[1]*Department of Civil Engineering, Zhejiang University, Hangzhou, China*

[2]*Institute for Infrastructure and Environment, School of Engineering, University of Edinburgh, Scotland, UK*

[3]*Department of Civil Engineering, The University of Hong Kong, Pokfulam Road, Hong Kong, China*

Abstract

A finite element analysis and design of austenitic and duplex stainless steel tubular section beam-columns is presented in this paper. The nonlinear finite element model was verified against experimental results of stainless steel tubular section beam-columns and beams. In this study, square and rectangular hollow sections were investigated. It was shown that the finite element model closely predicted the ultimate loads and failure modes of the tested beam-columns and beams. Hence, the finite element model was used for an extensive parametric study. The axial compressive strengths of the beam-column specimens predicted by the finite element analysis are compared with the design strengths calculated using the linear interaction equation and direct strength method. Reliability analysis was performed to assess the reliability of these design rules. It is shown that these design rules generally provide accurate and reliable predictions for stainless steel tubular section beam-columns. Design recommendations for linear interaction equation and the direct strength methods are proposed for stainless steel SHS and RHS beam-columns.

Keywords

Beam-columns; direct strength method; finite element analysis; rectangular and square hollow sections; stainless steel.

* Corresponding author. Tel.: +44 (0) 131 650 5736; Fax: +44 (0) 131 650 6554.

E-mail address: Yuner.Huang@ed.ac.uk

1 Introduction

Stainless steel sections have been increasingly used in building construction because of their superior corrosion resistance, ease of maintenance, and pleasing appearance. Therefore, considerable research has been carried out to investigate the structural behaviour of stainless steel members. Considerable experimental and numerical investigation on stainless steel compressive members [1-11] and flexural members [3, 12-17] has been performed. However, investigations on stainless steel beam-column members subjected to combined axial compression and bending are limited. Tests on beam-column members of austenitic stainless steel (EN 1.4301) were conducted by Talja and Salmi [18] and Kouhi et al. [19] on rectangular hollow sections (RHS), Burgan et al. [20] on I-sections, and Macdonald et al. [21] on lipped channel sections. Lui et al. [22] conducted a series of tests on cold-formed duplex stainless steel square hollow sections (SHS). Huang and Young [23, 24] and Zhao et al. [25, 26] investigated the beam-column behaviour of lean duplex stainless steel SHS and RHS. Arrayago et al. [27, 28] conducted experimental study on ferritic stainless steel beam-columns, in order to assess current design rules for stainless steel beam-column members. The test results of ferritic stainless steel beams [29], stub columns [30] were also used in comparing with design specifications. Zhao et al. [31 – 37] performed comprehensive study on stainless steel tubular beam-column members, covering ferritic stainless steel, austenitic stainless steel and duplex stainless steel. Investigations on equal and unequal end moments were conducted. Several design recommendations were proposed for stainless steel beam-column tubular members. Arrayago et al. [27] examined various design proposals based on direct-strength method (DSM) for stainless steel hollow cross-section beam-column members, and proposed a full slenderness range DSM approach based on experimental and numerical results. The proposed DSM is capable of incorporating strain hardening for stainless steel materials and the actual stress distribution of the cross-section when determining the elastic buckling stress.

Recently, finite element analysis has been widely used to investigate the behaviour of stainless steel members [4, 11, 17, 24, 26, 38]. Finite element analysis (FEA) is relatively inexpensive and time efficient compared with physical experiments, especially when a parametric study of cross-section geometries is involved. Although FEA is a useful and powerful tool for structural analysis and design, it is important to obtain an accurate and reliable finite element model (FEM) prior to a parametric study of FEA to be carried out. Therefore, one of the purposes of this study is to develop accurate finite element models for stainless steel tubular section beam-columns and beams.

The direct strength method specified in the North American Specification [39, 40] and Australian/New Zealand Standard [41] for cold-formed steel structures was developed by Schafer and Peköz [42] and Schafer [43]. It presents a competitive alternative to existing effective section methods as it obviates lengthy effective width calculations [44]. The current direct strength method

specified in the North American Specification [39, 40] and Australian/New Zealand Standard [41] is applicable for determination of the nominal axial and flexural strength of cold-formed steel members only. Rasmussen [44] applied the direct strength method to plain equal angel section beam-columns. Schafer [45] has considered the direct strength method for the design of short length of lipped channel section beam-columns and accounted for local and distortional buckling. Duong and Hancock [46] applied the direct strength method to long lipped channel beam-columns with the consideration of second order bending effect. In this study, the behaviour and design of stainless steel tubular section on duplex (EN 1.4462) and austenitic (EN 1.4301) stainless steel beam-columns and beams were investigated using finite element analysis. A finite element model is developed and validated with the beam-column tests conducted by Lui et al. [22] and beam tests conducted by Zhou and Young [12]. The beam-column strengths obtained from the finite element analysis are compared with design strengths predicted by linear load-moment interaction curves and direct strength method for beam-column that described in Arrayago et al. [27], with the compressive strength and flexural strength calculated by different design approaches.

2 Development of Finite Element Model

2.1 General

In this study, two different finite element models were developed using ABAQUS [47] for stainless steel beam-columns and beams, respectively. The four-node doubly curved shell element with reduced integration and hourglass control (S4R5) was used in the both two models. The element has five degree of freedom per node. The element allows for transverse shear deformation. In order to choose the finite element mesh that provides accurate results with minimum computational time, convergence studies were conducted. It is found that a 10 mm×10 mm (length by width) ratio provides adequate accuracy in modelling the columns. The material properties and stress-strain curves obtained from the tensile coupon tests were used in the finite element model. Since the analysis of post buckling involves large inelastic strains, the nominal (engineering) stress-strain curve was converted to a true stress and logarithmic plastic strain curve. The true stress and plastic true strain are specified in ABAQUS [47].

2.2 Beam-column Model

In the simulation of beam-columns, two types of analysis were performed in the finite element analysis for buckling. The first analysis is known as eigenvalue analysis that estimates the buckling modes and loads. This analysis is a linear elastic analysis performed using the (*BUCKLE) procedure available in the ABAQUS library with the load applied within the step. For practical

purposes, only the lowest buckling mode predicted from the eigenvalue analysis is used. The second analysis is called load-displacement nonlinear analysis and follows the eigenvalue prediction.

The bearing plates at both ends of the beam-columns are modelled as rigid body. In general, a rigid body is a collection of nodes, element, and/or surfaces whose motion is governed by the motion of a single node, called the rigid body reference point. The relative positions of the nodes and elements that are parts of the rigid body remain constant in the simulation. Therefore, the constituent elements do not deform but can undergo large rigid body motions. Since the motion of a rigid body can be prescribed by applying boundary conditions at the rigid body reference node, the restraints were applied on the reference point of the rigid body in this study. The reference point at the loaded end was restrained against x and y directions displacement and x-axis rotation but free to rotate about the y-axis. The reference point at another end was restrained against x, y and z directions displacement and x-axis rotation but free to rotate about the y-axis. The warping at the ends of the column was restrained. The nodes other than the two ends were free to translate and rotate in any direction.

The load was applied in increments using the modified RIKS method available in the ABAQUS library. The RIKS method is generally used to predicted unstable and nonlinear collapse of a structure such as postbuckling analysis. It uses the load magnitude as an additional unknown and solves simultaneously for loads and displacements. The nonlinear geometry parameter (NLGEOM) was included to deal with the large displacement analysis. The load was applied at the reference point of the loaded end. The loading eccentricity of beam-column was modeled as the distance from the reference point to the centroid of the specimen sections.

Both initial local and overall geometric imperfections are found in the beam-columns as a result of the fabrication process. Hence, superposition of local buckling mode as well as overall buckling mode with the measured magnitudes is recommended for accurate finite element analysis. These buckling modes could be obtained by carrying eigenvalue analysis of the column with very large value of plate width-to-thickness (b/t) ratio and very small value of b/t ratio to ensure local buckling and overall buckling occur, respectively. Only the lowest buckling mode (eigenmode 1) is used in the eigenvalue analysis. Since all buckling modes predicted by ABAQUS eigenvalue analysis are generalized to 1.0, the buckling modes are factored by the measured magnitudes of the initial local and overall geometric imperfections. The global imperfections for beam-column specimens were $L/939$ and $L/1883$ for sections S1 (40×40×2) and S2 (50×50×1.5) respectively, where L is the specimen length. The local imperfections of the beam-column specimens were 0.113 and 0.164 mm for sections S1 and S2, respectively.

2.3 Beam Model

In the simulation of beams, only half of the specimen was modeled for the symmetry. The support plate was modeled as a rigid surface, whose motion is governed by the reference point. The reference point of the support plate was restrained against *x*, *y* and *z* directions displacement as well as *y*- and *z*- axes rotation but free to rotate about the *x*-axis. The loading plate was also modeled as a rigid surface. The reference point of the loading plate was restrained against *x* and *z* directions displacement as well as *y*- and *z*- axes rotation but free to move in *y* directions and rotate about the *x*-axis. The constraint between the loading/support plate and specimen was simulated using contact surface. The web stiffener plates which stiffen the section at the load and support points were simulated by increasing the approximate 70% thickness of the elements at the corresponding parts. Thus the local failure at the loading and support points was prevented. The load was applied at the reference point of the loading plate. The nonlinear geometry parameter (NLGEOM) was included to deal with the large displacement analysis.

3 Verification of Finite Element Model

3.1 Beam-columns

The stainless steel beam-columns tested by Lui et al. [22] were used to validate the beam-column finite element model in this study. A beam-column test program on stainless steel tubular section specimens has been conducted by Lui et al. [22]. The tests were performed on two square hollow sections of duplex stainless steel. The test specimens were cold-rolled from annealed flat trips. The SHS had nominal dimension of 40 by 40 mm with thickness of 2 mm and 50 by 50 mm with thickness of 1.5 mm. The specimens were supplied from the manufacturer in uncut lengths of 3400 mm, and were cut into two different lengths of 550 mm and 1100 mm. Both ends were welded to carbon steel end plates to ensure full contact between specimen and end bearings. The test series were different by their cross-section dimensions and column lengths, testing at various eccentricities between pinned ends. Table 1 shows the average measured cross-section dimensions of the test specimens using the nomenclature defined in Fig. 1. The material properties were obtained from the coupon tests conducted by Young and Lui [48], as summarized in Table 2. The initial overall and geometric imperfections of the specimens were measured by Lui et al. [22] prior to testing. The average overall minor axis flexural imperfections at mid-length were 1/939 and 1/1883 of the specimen length for Series S1L2 and S2L2 respectively. The maximum initial local geometric imperfections of the specimens were 0.113 and 0.164 mm for section S1 (40×40×2) and S2 (50×50×1.5), respectively. In the finite element model (FEM), the measured cross-section dimensions, material properties and initial geometric imperfections from the tests were modeled. The

measured overall geometric imperfections at mid length for minor axis flexural imperfection at mid-length were 1/939 and 1/1883 of the specimen length for Series S1 and S2 respectively, as reported by Lui et al. [22]. The maximum initial local geometric imperfections of the specimens were 0.113 and 0.164 mm for Series S1 and S2 respectively [22].

The load capacity of the stainless steel tubular section beam-columns obtained from the finite element analysis are compared with the test results conducted by Lui et al. [22] in Table 3. Comparison of experimental and FEA deformed shape for specimen S1L2E10 is shown in Fig. 2. A maximum difference in load capacity of 5% was observed between test and numerical results for beam-column specimens of S2L1E00, S2L1E60, S2L2E25 and S2L2E60. The mean values of the load capacity ratios (N_{TEST}/N_{FEA}, $M_{end\text{-}TEST}/M_{end\text{-}FEA}$) are 0.99 with the corresponding coefficients of variation (COV) of 0.031. The comparison indicates that the load capacity of beam-column predicted by the FEA is accurate. The failure modes obtained from the test results and FEA for each specimen are also compared in Table 3. The observed failure modes included local buckling (L) and flexural buckling (F). The failure modes observed from the finite element analysis are in good agreement with those observed in the tests, except for the specimens S2L2E60. Figs. 3 and 4 show a good agreement of the load-deflection curves and load-rotation curves obtained from the test and FEA predictions for the Series S1L1, respectively. It is shown that both the load-defection and load-rotation relationships reflect good agreement between test and finite element results. Generally, it is shown that the finite element model is accurate and reliable.

3.2 Beams

The stainless steel beams tested by Zhou and Young [12] were modeled in this study, as shown in Fig. 5. Zhou and Young [12] performed a series of bending tests on cold-formed stainless steel square and rectangular hollow sections. The specimens were cold-rolled from austenitic stainless steel type 304, high strength austenitic (HSA) and duplex steel sheets. The stainless steel type 304 is considered as normal strength material, whereas the HSA and duplex are considered as high strength material. The specimens consisted of 15 different section sizes, having nominal thickness (t) ranging from 1.5 to 6 mm, nominal overall depth of the webs (B_w) from 40 to 200 mm, and nominal flange widths (B_f) from 40 to 150 mm. The length of the specimens was chosen such that the section moment capacity could be obtained. Table 4 shows the measured specimen dimensions for the test specimens, using the nomenclature defined in Fig. 1. The material properties obtained from the coupon tests and ultimate load of the test specimens are summarized in Table 4. The measured cross-section dimensions and material properties reported in Table 4 were incorporated in the finite element model. The ultimate moments of the stainless steel beams obtained from the finite element analysis are compared with the test results conducted by Zhou and Young [12] in Tables 5. A maximum difference in ultimate moments of 7% was observed between test and numerical results for

beam specimen of N120×60×2. The mean value of the ultimate moment ratio (M_{TEST}/M_{FEA}) is 0.97 with the corresponding coefficient of variation (COV) of 0.025. The comparison indicates that the ultimate moments of beams predicted by the FEA are accurate.

4 Parametric Study

The verification showed that the finite element models reasonably accurate for predicting the strengths of stainless steel tubular section beam-columns and beams. Hence, parametric study was carried out to investigate the behaviour of stainless steel tubular section beam-columns and beams. In the parametric study, four kinds of sections, namely 100×50×2, 150×100×2, 100×100×2 and 180×180×3 having different length of 1400 and 2800 mm were studied. The cross section dimensions are shown in Table 6, using the nomenclature defined in Fig. 1. The specimens used in parametric analysis were designed to investigate various geometric parameters. The outer web width and outer flange width ranged from 50 mm to 180 mm, having aspect ratio equal to 1, 1.5 and 2. The local slenderness (λ_l) ranged from 1.0 to 2.0, and the generalized slenderness (λ_n) ranged from 1.04 to 1.99, covering a wide range of slender cross sections. The global slenderness (λ_c) covered a wide range of 0.3 to 2.5. The length of bearing plates at both ends of the specimens was assumed as 40 mm. Two kinds of stainless steel materials, namely high strength stainless steel grade EN 1.4462 (Duplex) and normal strength stainless steel grade EN 1.4301 (AISI 304), were used in the parametric study. Material tests of stainless steel EN 1.4462 and EN 1.4301 were conducted by Chen and Young [49]. The material properties in flat portion of the sections obtained from tensile coupon tests were adopted in parametric study, which are summarized in Table 7.

Different eccentricities were considered for each specimen. The specimens are separated into eight series according to their material properties, section dimension and specimen length. The specimens are labeled such that the material properties, section dimension, specimen length and eccentricity could be identified from the label. For example, the labels "HS100×50×1400E30" define the specimens having high strength material and nominal overall depth of the web of 50 mm, overall flange width of 100 mm, and length of 1400 mm with the eccentricity of 30 mm; the labeled 'NS100×100×2800E60' defines the specimen having normal strength material and nominal overall depth of the web of 100 mm, overall flange width of 100 mm, and length of 2800 mm with eccentricity of 60 mm. The normalized radius of beam-column strength (r_{FEA}) obtained from numerical analysis is used to compare with the corresponding design strength (r_d), which is calculated by Eq (1), and as shown in Fig 6.

$$r_{FEA} = \sqrt{\left(\frac{P_{FEA}}{P_y}\right)^2 + \left(\frac{P_{FEA}\times e}{M_y}\right)^2}, \quad r_d = \sqrt{\left(\frac{P_d}{P_y}\right)^2 + \left(\frac{P_d\times e}{M_y}\right)^2} \tag{1}$$

5 Design Rules and Comparison of Design Strengths

5.1 General

In this study, the nominal strengths (unfactored design strengths) of the stainless steel beam-columns were calculated using linear interaction equation for beam-columns, and direct strength method (DSM) for stainless steel and carbon steel beam-columns proposed by Arrayago et al. [27]. The bending moment capacity (M_n) and axial loading capacity (P_n) of effective sections, as well as the bending moment capacity (M_{ne}) and axial loading capacity (P_{ne}) of fully effective sections, were calculated by ASCE Specification [50], DSM in AISI [39] and DSM modified by Huang and Young [24]. Therefore, nine design methods are evaluated in this study. The cross-section dimensions and material properties used in the parametric study were adopted in the calculation of design strengths. The design strengths were compared with the numerical results obtained from the parametric study, and thus the suitability of the existing design rules were assessed. Comparison of FEA results with design strength of beam-column members is shown in Table 8. Prediction for column and beam strength is important for the accuracy in predicting beam-column strengths. Table 9 summarizes comparison of FEA results with design strengths of column members and beam members.

5.2 Linear interaction equation and effective width method

Design strength of stainless steel beam-column members are calculated by load-moment interactive equation in the ASCE Specification [50]. Linear load-secondary moment interaction equation, as shown in Eq (2), is used to predict the unfactored design axial strength P_u for beam-columns is calculated by the following interaction equations:

$$\frac{P_u}{P_n} + C_m k \frac{M_{end,u}}{M_n} \leq 1.0 \tag{2}$$

where $M_{end,u}$ is the end moment corresponding to the design strength, $M_{end,u} = P_u \times e_p$; k is the amplification factor = $1/(1-P_u/P_{ey})$; P_{ey} is the elastic flexural buckling load; C_m is the coefficient for unequal end moment; P_n is the member strength in compression; and M_n is the flexural strength of member. Therefore, the design strength of beam-column members (P_u) largely depends on the prediction of member strength in compression (P_n) and bending (M_n). In this Section, P_n and M_n are calculated by ASCE [50], DSM in AISI [39], and modified DSM in Huang and Young [24], in

determining beam-column strength (P_u). Comparison of FEA results with design strengths calculated by linear interaction load-moment curve for Series HS100-50-1400 is shown in Fig. 7.

5.2.1 P_n and M_n determined by ASCE [50]

According the ASCE Specification, the column strength $P_n = A_e F_n$, where A_e is effective area, and F_n is buckling strength. F_n is calculated by Eq (3), where E_t is tangent modulus at F_n, as shown in Eq (4). Therefore, the calculation of buckling strength F_n involves an iterative process. The inelastic reserve capacity approach in ASCE Specification is used to calculate M_n, according to the procedure II in Clause 3.3.1.1 in ASCE Specificaion [50].

$$F_n = \frac{\pi^2 E_t}{(KL/r)^2} \leq F_y \tag{3}$$

$$E_t = \frac{E_o F_y}{F_y + 0.002 n E_o \left(\frac{F_n}{F_y}\right)^{n-1}} \tag{4}$$

The normalized design strengths of beam-column members (r_{ASCE}) calculated by linear interaction curve, in which P_n and M_n are determined using the ASCE Specification, are compared with the numerical results of austenitic stainless steel and duplex stainless steel tubular section beam-columns, as shown in Table 8. Generally, it is shown that the ASCE Specification provides accurate predictions for stainless steel tubular section beam-columns. It is observed that the FEA-to-design strength ratios (r_{FEA}/r_{ASCE}) equal to 0.99, 0.98 and 0.99, with coefficient of variation (COV) of 0.106, 0.110 and 0.108, for duplex stainless steel material (HS), austenitic stainless steel material (NS) and for all 158 specimens, respectively, as shown in Table 8. The unfactored design compressive strength for columns (P_{ASCE}) and flexural strengths (M_{ASCE}) are compared with the numerical results of stainless steel column and beam members, as summarized in Table 9. It is shown that the ASCE Specification provides unconservative prediction for columns with mean P_{FEA}/P_{ASCE} for all specimens are 0.85 with COV of 0.098. The prediction for flexural strength is conservative, with mean value of M_{FEA}/M_{ASCE} for all specimens equals to 1.11 with COV of 0.055, respectively.

5.2.2 P_n and M_n determined by DSM in AISI [39]

The normalized design strength of beam-column members (r_{DSM}) was calculated by linear interaction curve (Eq 2), in which P_n and M_n were determined using AISI S100 Specification. The column strength P_n is calculated by Eqs (5 – 6), where λ_c and λ_l are the non-dimensional slenderness for P_{ne} and P_n, respectively, based on the clause 1.2.1.1 of Appendix 1 of AISI S100 Specification.

$$P_{ne} = \begin{cases} \left(0.658^{\lambda_c^2}\right)P_y & for\ \lambda_c \leq 1.5 \\ \left(0.877/\lambda_c^2\right)P_y & for\ \lambda_c > 1.5 \end{cases} \quad (5)$$

$$P_n = \begin{cases} P_{ne} & for\ \lambda_l \leq 0.776 \\ \left[1-0.15(P_{crl}/P_{ne})^{0.4}\right](P_{crl}/P_{ne})^{0.4}P_{ne} & for\ \lambda_l > 0.776 \end{cases} \quad (6)$$

The flexural capacity M_n is calculated by Eq (7), where $\lambda_l = (M_{ne}/M_{crl})^{0.5}$. According to Clause 1.2.2.2 in the Appendix 1 of Commentary of the AISI S100 Specification [40], the M_{ne} is taken as the yield moment (M_y).

$$M_n = \begin{cases} M_{ne} & for\ \lambda_l \leq 0.776 \\ \left[1-0.15(M_{crl}/M_{ne})^{0.4}\right](M_{crl}/M_{ne})^{0.4}M_{ne} & for\ \lambda_l > 0.776 \end{cases} \quad (7)$$

The comparison between numerical results (r_{FEA}) and design strengths (r_{DSM}) is shown in Table 8. It is noted that this design method is capable of providing accurate and convergent prediction for stainless steel beam-column members. The mean value of r_{FEA}/r_{DSM} is 1.06 and 1.04 for duplex (HS) and austenitic (NS) stainless steel members, with COV equals to 0.093 and 0.088, respectively. Considering all of the 158 specimens, the mean value of r_{FEA}/r_{DSM} is 1.05, with COV of 0.091. In addition, the calculation procedure for P_n and M_n with this design approach is more convenient than the design approach described in Section 6.2.1. It is shown in Table 9 that the direct strength method in AISI provided slightly conservative prediction for column strength, with a mean value of P_{FEA}/P_{DSM} equals to 1.06 with COV of 0.073 for all specimens. It provides quite conservative prediction for flexural capacity, with a mean value of M_{FEA}/M_{DSM} = 1.15 and COV = 0.060.

5.2.3 P_n and M_n determined by Huang and Young [24]

The normalized design strength of beam-column members ($r_{H\&Y}$) was calculated by linear interaction curve (Eq 2), in which P_n and M_n were calculated with a modified direct strength method proposed in Huang and Young [24]. The column strength P_n is calculated by Eqs (8 – 9), and M_n is calculated by Eqs (10), where $M_{ne} = M_y$. The notations are the same as the direct strength method described in Section 5.2.2.

$$P_{ne} = \begin{cases} \left(0.87^{\lambda_c^2}\right)P_y & for\ \lambda_c \leq 1 \\ \left(0.877/\lambda_c^2\right)P_y & for\ \lambda_c > 1 \end{cases} \quad (8)$$

$$P_n = \begin{cases} P_{ne} & for\ \lambda_l \leq 0.769 \\ \left[1-0.16(P_{crl}/P_{ne})^{0.4}\right](P_{crl}/P_{ne})^{0.4}P_{ne} & for\ \lambda_l > 0.769 \end{cases} \quad (9)$$

$$M_n = \begin{cases} 1.1((0.776-\lambda_l)+1)M_{ne} & for\ \lambda_l \leq 0.776 \\ \left[1-0.15\left(\frac{M_{crl}}{1.1M_{ne}}\right)^{0.4}\right]\left(\frac{M_{crl}}{1.1M_{ne}}\right)^{0.4}1.1M_{ne} & for\ \lambda_l > 0.776 \end{cases} \quad (10)$$

The comparison between numerical results (r_{FEA}) and design strengths ($r_{H\&Y}$) is summarized in Table 8. It shows that this design approach provides the best design strength prediction among the three approaches with linear interaction curve. The mean values of $r_{FEA}/r_{H\&Y}$ are 1.01, 0.98 and 0.99 duplex stainless steel, austenitic stainless steel members, and all specimens, respectively, which are quite close to unity. The corresponding COVs are relatively small, which are 0.099, 0.100 and 0.101, respectively. Similar to the direct strength method in AISI, the calculation procedure for P_n and M_n with Huang and Young [24] is more convenient than ASCE [50]. Therefore, it is shown that linear interaction curve with P_n and M_n calculated by Huang and Young [24] provides accurate design method with convenient calculation procedure.

The accurate prediction for beam-column strength ($r_{H\&Y}$) by this design approach is partly due to its accurate prediction for column strength ($P_{H\&Y}$) and flexural strength ($M_{H\&Y}$), which are the two anchor points in the linear interaction curve. It is shown in Table 9 that the mean values of $P_{FEA}/P_{H\&Y}$ and $M_{FEA}/M_{H\&Y}$ equal to 1.00 and 1.08, with COV of 0.085 and 0.061, for all specimens. It provides quite conservative prediction for flexural capacity, with a mean value of M_{FEA}/M_{DSM} = 1.15 and COV = 0.060. Predictions for column strength and flexural strength by Huang and Young [24] are the most accurate among the three approaches with linear interaction curve.

5.3 Direct Strength Method for Beam-Columns Proposed by Arrayago et al. [27]

Arrayago et al. [27] proposed two direct strength equations of beam-column members for carbon steel and stainless steel materials, in which local buckling and enhanced material strength are considered. Therefore, calculation of effective area is not required, as the local buckling effect is considered through direct strength curve. The direct strength equations for the normalized design strength for beam-column member of carbon steel (r_{cs}^*) and stainless steel (r_{ss}^*) are shown in Eq. 11 and Eq 12, respectively:

$$\frac{r_{cs}^*}{r_{ne}} = \begin{cases} 1+(1-1.29\lambda_n)\left(\frac{\sigma_u}{\sigma_{0.2}}-1\right) & for\ \lambda_n \leq 0.776 \\ \frac{1}{\lambda_n^{0.8}}-\frac{0.15}{\lambda_n^{1.6}} & for\ \lambda_n > 0.776 \end{cases} \tag{11}$$

$$\frac{r_{ss}^*}{r_{ne}} = \begin{cases} 1+(1-2.11\lambda_n)\left(\frac{\sigma_u}{\sigma_{0.2}}-1\right) & for\ \lambda_n \leq 0.474 \\ \frac{0.95}{\lambda_n^{0.8}}-\frac{0.22}{\lambda_n^{1.6}} & for\ \lambda_n > 0.474 \end{cases} \tag{12}$$

where σ_u and $\sigma_{0.2}$ are ultimate strength and 0.2% proof strength (yield strength) of steel material, and r_{ne} and λ_n are calculated with Eqs 13 – 16:

$$\frac{P_{one}}{P_{ne}} + k \cdot C_m \frac{M_{one}}{M_{ne}} = 1 \tag{13}$$

$$r_{ne} = \sqrt{\left(\frac{P_{one}}{P_y}\right)^2 + \left(\frac{M_{one}}{M_y}\right)^2} \quad (14)$$

$$r_{crl} = \sqrt{\left(\frac{P_{ocr}}{P_y}\right)^2 + \left(\frac{M_{ocr}}{M_y}\right)^2} \quad (15)$$

$$\lambda_n = \sqrt{\frac{r_{ne}}{r_{crl}}} \quad (16)$$

where P_{ne} is the flexural buckling resistance of the fully effective column; M_{ne} is the bending moment capacity of the fully effective member; P_{ocr} and M_{ocr} are the axial compression and moment causing local buckling under combined compression and bending loading conditions, obtained from a buckling analysis [51]; N_{one} and M_{one} are the overall buckling strength for column and beam, respectively; and P_y and M_y are the squash load and yield moment, respectively. It is noted from Eqs 11 – 16 that the calculation for beam-column strength varies with different design approaches to calculate P_{ne} and M_{ne}. Therefore, in this paper, three design approaches (ASCE [50], DSM [39] and Huang and Young [24]) to calculate P_{ne} and M_{ne} are used, and the corresponding design strength of beam-column members are compared to assess suitability of various design approaches. It should be noted that these design approaches are not covered in Arrayago et al. [27], and thus it complements Arrayago et al. [27] in assessing suitability of design rules for stainless steel beam-columns.

5.3.1 P_{ne} and M_{ne} determined by ASCE [50]

The direct strength methods proposed by Arrayago et al. [27] was used, in which P_{ne} and M_{ne} were calculated by ASCE [50]. The flexural buckling resistance of the fully effective column $P_{ne} = A \times F_n$, where A is full cross-sectional area, and F_n is buckling strength that calculated by Eq 3. The inelastic reserve capacity approach in ASCE Specification is used to calculate M_{ne}, and the calculation is based on a fully effective cross-section.

The normalized design strengths of beam-column members that calculated by the direct strength method for carbon steel (Eq. 11) and stainless steel (Eq. 12) are represented by $r^*_{cs,ASCE}$ and $r^*_{ss,ASCE}$, respectively. Comparison between numerical strength and design strength is shown in Table 8, Fig 8 and Fig 9. Generally, it is shown that the direct strength method with P_{ne} and M_{ne} calculated by ASCE [50] provides unconservative and scatter predictions for stainless steel tubular section beam-columns. The FEA-to-design strength ratios for carbon steel curve ($r_{FEA}/r^*_{cs,ASCE}$) equal to 0.87, 0.76 and 0.82, with coefficient of variation (COV) of 0.201, 0.318 and 0.267, for duplex stainless steel (HS), austenitic stainless steel (NS) and for all 158 specimens, respectively. The FEA-to-design

strength ratios for stainless steel curve ($r_{FEA}/r^*_{ss,ASCE}$) equal to 0.98, 0.88 and 0.93, with coefficient of variation (COV) of 0.207, 0.334 and 0.277, for HS, NS and for all specimens, respectively.

5.3.2 P_{ne} and M_{ne} determined by DSM in AISI [39]

The normalized design strength of beam-column members ($r^*_{cs,DSM}$ and $r^*_{ss,DSM}$) were calculated by direct strength method proposed by Arrayago et al. [27] (Eqs 11 and 12), in which P_{ne} was obtained by Eq. (5) and $M_{ne} = M_y$, according to the direct strength method for compressive members and flexural members in AISI S100 Specification. The comparison between numerical results (r_{FEA}) and design strengths is summarized in Table 8, Fig 8 and Fig 9. It is shown that the carbon steel curve provides accurate and convergent prediction for stainless steel beam-column tubular members, while the stainless steel curve is quite conservative.

The FEA-to-design strength ratios for carbon steel curve ($r_{FEA}/r^*_{cs,DSM}$) equal to 1.01, 0.99 and 1.00, with coefficient of variation (COV) of 0.088, 0.064 and 0.078, for duplex stainless steel, austenitic stainless steel and all specimens, respectively. Overall, the direct strength method proposed by Arrayago et al. [27] with P_{ne} and M_{ne} calculated by DSM in AISI [39] provides the best prediction for stainless steel beam-column members investigated in this study. The FEA-to-design strength ratios for stainless steel curve ($r_{FEA}/r^*_{ss,DSM}$) equal to 1.16, 1.15 and 1.15, with coefficient of variation (COV) of 0.085, 0.069 and 0.077, for duplex stainless steel, austenitic stainless steel and all specimens, respectively.

5.3.3 P_{ne} and M_{ne} determined by Huang and Young [24]

According to Huang and Young [24], P_{ne} is obtained by Eq. (8), and $M_{ne} = 1.1 \times M_y$. The normalized design strength of beam-column members ($r^*_{cs,H\&Y}$ and $r^*_{ss,H\&Y}$) were calculated by direct strength method proposed by Arrayago et al. [27] (Eqs 11 and 12). The comparison between numerical results (r_{FEA}) and design strengths is summarized in Table 8, Fig 8 and Fig 9. Compared with the previous design rule described in Section 6.3.2, this design approach provides less conservative prediction. Generally speaking, the carbon steel curve provides slightly unconservative prediction and the stainless steel curve provides conservative prediction for stainless steel beam-column tubular members.

The FEA-to-design strength ratios for carbon steel curve ($r_{FEA}/r^*_{cs,H\&Y}$) equal to 0.97, 0.93 and 0.95, with coefficient of variation (COV) of 0.091, 0.066 and 0.082, for duplex stainless steel, austenitic stainless steel and all specimens, respectively. The FEA-to-design strength ratios for stainless steel curve ($r_{FEA}/r^*_{ss,H\&Y}$) equal to 1.10, 1.08 and 1.09, with coefficient of variation (COV) of 0.089, 0.076 and 0.083, for duplex stainless steel, austenitic stainless steel and all specimens, respectively.

6 Reliability Analysis

Reliability analysis detailed in the Commentary of the ASCE Specifications [50] is used to assess reliability of various design rules in this study. The result of reliability analysis is shown in Table 8. A target reliability index of 2.5 for stainless steel structural members is used as a lower limit in this study. The design rules are considered to be reliable if the reliability index is greater than or equal to the target value. The resistance factors (ϕ) of 0.85 was used in calculating the reliability index (β). The load combinations of 1.2DL+1.6LL was adopted in this study, as specified in ASCE [52], where DL is the dead load and LL is the live load. The mean-to-nominal ratio and coefficient of variation considered for different materials of 1.10 and 0.10 were used in this study, respectively. The mean-to-nominal ratio and coefficient of variation considered for different geometries of 1.00 and 0.05 were used, respectively. These values are adopted according to the Clause 3.3.1.1 of the commentary of the ASCE Specification for compression and flexural members. The correction factor (C_p) as shown in Eq. F1.1-4 of the AISI S100 Specification [39] was used to account for the influence due to a small number of data in calculating the reliability index.

It is shown that the three design approaches using linear interactive equations for beam-column specimens (r_{ASCE}, r_{DSM}, $r_{H\&Y}$) are considered to be reliable, as the reliability index for duplex stainless steel, austenitic stainless steel and all specimens are higher than the target value of 2.5. The reliability of direct strength method proposed by Arrayago et al. [27] depends largely on the calculation of P_{ne} and M_{ne}, and the direct strength curve adopted. When the P_{ne} and M_{ne} were determined with ASCE Specification [50], it is shown that the reliability index (β) for the carbon steel curve ($r^*_{CS,ASCE}$) and the stainless steel curve ($r^*_{SS,ASCE}$) are consistently smaller than 2.5. Therefore, this design approach is considered not reliable for stainless steel beam-column members, with resistance factor of 0.85. When the P_{ne} and M_{ne} were determined with direct strength method is AISI [39], the reliability index (β) for the carbon steel and stainless steel curves are both higher than 2.50. Thus this design approach is considered reliable with resistance factor (ϕ) of 0.85. When the P_{ne} and M_{ne} were determined by Huang and Young [24], the reliability index (β) for the carbon steel curve are higher than the target value of 2.50 for duplex stainless steel, but it is smaller than 2.50 for austenitic stainless steel and for all specimens. The reliability index (β) for the stainless steel curve are all higher than 2.50. Thus, this design approach is considered reliable with resistance factor (ϕ) of 0.85 when the stainless steel curve is used.

7 Conclusions

The paper presents a finite element analysis and design of stainless steel tubular section beam-columns and beams. Finite element models including geometric and material non-linearities have been developed and verified against experimental results. The failure modes at ultimate load predicted by the finite element analysis were generally in good agreement with the failure modes observed in the tests. In addition, the load-deflection curves and load-rotation curves predicted by the finite element analysis also agree well with the test results. The finite element models provided good predictions of the experimental ultimate loads for the stainless steel tubular section beam-columns and beams. Hence, a parametric study on stainless steel tubular section specimens has been performed using the developed finite element model for beam-columns. Four kinds of sections having different length of 1400 and 2800 mm were studied with a wide range of slenderness, while both the high strength and normal strength stainless steel material were considered.

The finite element analysis results were compared with the design strengths calculated using various design approaches based on linear load-moment interaction curve and direct strength method proposed in Arrayago et al. [27]. Generally, it is shown that the linear load-moment interaction curve provides accurate and reliable prediction for stainless steel beam-column members when the P_n and M_n value are obtained from ASCE [50], DSM in AISI [39] and Huang & Young [24]. It is shown that Huang and Young [24] provides the best prediction among the three design approaches using linear interaction curve presented in this study. The direct strength method for carbon steel proposed by Arrayago et al. [27] for beam-column members is quite unconservative when the P_{ne} and M_{ne} are calculate by ASCE, and slightly conservative when the P_{ne} and M_{ne} are calculated by Huang & Young [24]. However, the direct strength method for carbon steel proposed by Arrayago et al. [27] provides the best prediction among all design approaches in this study when the P_{ne} and M_{ne} are calculated by DSM in AISI [39]. The direct strength method for stainless steel in Arrayago et al. [27] is unconservative when the P_{ne} and M_{ne} are calculate by ASCE, and quite conservative when the P_{ne} and M_{ne} are calculated by DSM in AISI [39] and Huang & Young [24]. Considering the accuracy, reliability and convenience in calculation procedure, it is recommended that the linear interaction equation with modified direct strength method proposed by Huang and Young [24], and the direct strength method for carbon steel proposed by Arrayago et al. [27] provides the best prediction among all design approaches in this study when the P_{ne} and M_{ne} are calculated by DSM in AISI [39] are used for stainless steel SHS and RHS beam-columns.

References

[1] Young B and Hartono W. "Compression Tests of Stainless Steel Tubular Members". *Journal of Structural Engineering*, *ASCE*, 2002; 128(6): 754-761.

[2] Liu Y and Young B. "Buckling of stainless steel square hollow section compression members". *Journal of Constructional Steel Research*, 2003; 59(2): 165-177.

[3] Gardner L and Nethercot DA. "Experiments on stainless steel hollow sections — Part 2: Member behavior of columns and beams". *Journal of Constructional Steel Research*, 2004; 60(9): 1319-1332.

[4] Ellobody E and Young B. "Structural performance of cold-formed high strength stainless steel columns". *Journal of Constructional Steel Research*, 2005; 61(12): 1631-1649.

[5] Ashraf M, Gardner L and Nethercot DA. "Compression strength of stainless steel cross-sections". *Journal of Constructional Steel Research*, 2006; 62(1-2): 105-115.

[6] Lecce M and Rasmussen KJR. "Distortional Buckling of Cold-Formed Stainless Steel Sections: Experimental Investigation". *Journal of Structural Engineering, ASCE*, 2006; 132(4): 497-504.

[7] Young B and Lui WM. "Tests of cold-formed high strength stainless steel compression members". *Thin-walled structures*, 2006; 44(2); 224-234.

[8] Rossi B, Jaspart JP and Rasmussen KJR. "Combined distortional and overall flexural-torsional buckling of cold-formed stainless steel sections: Experimental investigations." *Journal of Structural Engineering*, *ASCE*, 2010; 136(4): 354 – 360.

[9] Rossi B, Jaspart JP and Rasmussen KJR. "Combined distortional and overall flexural-torsional buckling of cold-formed stainless steel sections: Design". *Journal of Structural Engineering*, *ASCE*, 2010; 136(4): 361 – 369.

[10] Huang Y and Young B. "Tests of pin-ended cold-formed lean duplex stainless steel columns". *Journal of Constructional Steel Research*, 2013; 82: 203 - 215.

[11] Huang Y and Young B. "Structural performance of cold-formed lean duplex stainless steel columns". *Thin-Walled Structures,* 2014; 83: 59 – 69.

[12] Zhou F and Young B. "Tests of cold-formed stainless steel tubular flexural members". *Thin-walled structures*, 2005; 43(9); 1325-1337.

[13] Kiymaz G. "Strength and stability criteria for thin-walled stainless steel circular hollow section members under bending". *Thin-Walled Structures*, 2005; 43(10): 1534-1549.

[14] Real E and Mirambell E. "Flexural behaviour of stainless steel beams". *Engineering Structures*, 2005; 27(10): 1465-1475.

[15] Gardner L, Talja A and Baddoo NR. "Structural design of high-strength austenitic stainless steel". *Thin-walled structures*, 2006; 44(5); 517-528.

[16] Theofanous M, Chan TM and Gardner L. "Flexural behaviour of stainless steel oval hollow sections". *Thin-Walled Structures*, 2009; 47(6-7): 776-787.

[17] Huang Y and Young B. "Experimental and numerical investigation of cold-formed lean duplex stainless steel flexural members". *Thin-Walled Structures*, 2014; 73: 216 - 228.

[18] Talja A and Salmi P. "Design of stainless steel RHS beams, columns and beam-columns". 1995, VTT Building Technology, Finland.

[19] Kouhi J, Talja A, Salmi P and Ala-Outinen T. "Current R&D work on the use of stainless steel in construction in Finland". *Journal of Constructional Steel Research*, 2000; 54(1): 31-50.

[20] Burgan BA, Baddoo NR and Gilsenan KA. "Structural design of stainless steel members – comparison between Eurocode 3, Part 1.4 and test results". *Journal of Constructional Steel Research*, 2000; 54(1): 51-73.

[21] Macdonald M, Rhodes J and Kotelko M. "Stainless steel stub columns subject to combined bending and axial loading". *Thin-Walled Structures*, 2007; 45(10-11): 893-897.

[22] Lui WM, Ashraf M and Young B. "Tests of cold-formed duplex stainless steel SHS beam-columns", *Engineering Structures*, 2014; 74: 111-121.

[23] Huang Y and Young B. “Experimental investigation of cold-formed lean duplex stainless steel beam-columns”. *Thin-Walled Structures*, 2014; 76: 105 - 117.

[24] Huang Y and Young B. “Design of cold-formed lean duplex stainless steel members in combined compression and bending”. *Journal of Structural Engineering ASCE*. 2015; 141(5):04014138.

[25] Zhao O, Rossi B, Gardner L, Young B. “Behaviour of structural stainless steel cross-sections under combined loading – Part I: Experimental Study”, *Engineering Structures*, 2015; 89: 236-246.

[26] Zhao O, Rossi B, Gardner L, Young B. “Behaviour of structural stainless steel cross-sections under combined loading – Part II: Numerical modelling and design approach”, *Engineering Structures*, 2015; 89: 247-259.

[27] Arrayago I, Rasmussen KJR, Real E. “Full slenderness range DSM approach for stainless steel hollow cross-section columns and beam-columns”. *Journal of Constructional Steel Research*, 2017; 138: 246 – 263.

[28] Arrayago I, Real E, Mirambell E. “Experimental study on ferritic stainless steel RHS and SHS beam-columns”. *Thin-Walled Structures*, 2016; 100: 93 – 104.

[29] Arrayago I, Real E. “Experimental study on ferritic stainless steel simply supported and continuous beams”. *Journal of Constructional Steel Research*, 2016; 119: 50 – 62.

[30] Arrayago I, Real E. “Experimental study on ferritic stainless steel RHS and SHS cross-sectional resistance under combined loading”, *Structures*, 2015; 4: 69 – 79.

[31] Zhao O, Rossi B, Gardner L and Young B. “Experimental and numerical studies of ferritic stainless steel tubular cross-sections under combined compression and bending”. *Journal of Structural Engineering, ASCE*, 2016; 142(2): 04015110.

[32] Zhao O, Gardner L and Young B. "Structural performance of stainless steel circular hollow sections under combined axial load and bending – Part 1: Experiments and numerical modelling". *Thin-Walled Structures*, 2016; 101: 231–239.

[33] Zhao O, Gardner L and Young B. "Structural performance of stainless steel circular hollow sections under combined axial load and bending – Part 2: Parametric studies and design". *Thin-Walled Structures*, 2016; 101: 240–248.

[34] Zhao O, Gardner L and Young B. "Buckling of ferritic stainless steel members under combined axial compression and bending". *Journal of Constructional Steel Research*, 2016; 117: 35–48.

[35] Zhao O, Gardner L and Young B. "Experimental study of ferritic stainless steel tubular beam-column members subjected to unequal end moments". *Journal of Structural Engineering, ASCE*, 2016; 142(11): 04016091.

[36] Zhao O, Gardner L and Young B. "Behaviour and design of stainless steel SHS and RHS beam-columns". *Thin-Walled Structures*, 2016; 106: 330–345.

[37] Zhao O, Gardner L and Young B. "Testing and numerical modelling of austenitic stainless steel CHS beam-columns". *Engineering Structures*, 2016; 111: 263–274.

[38] Ashraf M, Gardner L and Nethercot DA. "Finite element modelling of structural stainless steel cross-sections". *Thin-walled structures*, 2006; 44(10): 1048-1062.

[39] "North American Specification for the design of cold-formed steel structural members". *AISI S100-16*, American Iron and Steel Institute and CSA Group, Washington, D.C.; 2016.

[40] "Commentary on North American Specification for the Design of Cold-Formed Steel Structural Members". *AISI S100-16-C*, American Iron and Steel Institute; Washington, D.C.; 2016.

[41] Australian/New Zealand Standard, "Cold-formed steel structures". *AS/NZS 4600:2005*, Standards Australia; Sydney, Australia; 2005.

[42] Schafer BW and Peköz T. "Direct strength prediction of cold-formed steel members using numerical elastic buckling solutions". *Proceedings of the 14th International Specialty Conference on Cold-Formed Steel Structures*, University of Missouri-Rolla, 1998; 69-76.

[43] Schafer BW. "Local, distortional, and Euler buckling of thin-walled columns". *Journal of Structural Engineering, ASCE*, 2002; 128(3): 289-299.

[44] Rasmussen KJR. "Design of slender angle section beam-columns by the direct strength method". *Journal of Structural Engineering, ASCE*, 2006; 132(2): 204-211.

[45] Schafer BW. "Advances in direct strength design of thin-walled members". *Proceedings of the International Conference on Advances in Structures: Steel, Concrete, Composite and Aluminum*, 2003; 333 - 340.

[46] Duong HM and Hancock GJ. "Recent developments in the direct strength design of thin-walled members". *Proceedings of the International workshop on recent advances and future trends in thin-walled structures technology*. J. Loughlan, Loughborough, Canopus, 2004; 43-62.

[47] ABAQUS analysis user's manual. Version 6.5. ABAQUS, Inc; 2004.

[48] Young B and Lui WM. "Behavior of cold-formed high strength stainless steel sections". *Journal of Structural Engineering, ASCE*, 2005; 131: 1738-45.

[49] Chen J and Young B. "Stress-strain curves for stainless steel at elevated temperatures". *Engineering Structures*, 2006; 28(2): 229-239.

[50] American Society of Civil Engineers (ASCE) Standard. "Specification for the design of cold-formed stainless steel structural members". American Society of Civil Engineers; *SEI/ASCE-8-02*, Reston, Virginia; 2002.

[51] Papangelis JP and Hancock GJ. "Computer analysis of thin-walled structural members". *Computer and Structures*, 1995; 56(1): 157-176.

[52] American Society of Civil Engineers (ASCE) Standard. "Minimum design loads for buildings and other structures", *ASCE/SEI 7-10*. Virginia; 2010.

Nomenclature

The following symbols are used in this paper:

A = gross area;

B_f = flange width of section;

B_w = web width of section;

C_m = coefficient for unequal end moment in ASCE specification;

e = amplified eccentricity;

e_p = loading eccentricity;

E = elastic modulus;

E_o = elastic modulus;

F_y = yield stress;

f_u = yield stress;

$f_{0.2}$ = yield stress;

L = column length;

N_{ASCE} = axial strength calculated using ASCE specification;

N_c = member strength in compression;

N_d = member strength calculated by design rules;

$N_{DSM,AISI}$ = axial strength calculated using direct strength method in AISI;

$N_{DSM,H\&Y}$ = axial strength calculated using modified direct strength method proposed by Huang and Young;

$N_{DSM,R}$ = axial strength calculated using direct strength method for beam-columns proposed by Rasmussen;

N_{ey} = Euler buckling load about the minor *y* axis;

N_{FEA} = axial strength obtained using FEA;

N_n = nominal compressive strength for compression members;

N_{ne} = least of the flexural, torsional and flexural torsional buckling load;

N_{ocr} = axial load buckling load;

N_{one} = overall axial capacity;

N_s = section strength in compression;

N_{TEST} = axial strength obtained from tests;

N_u = axial strength;

N_Y = squash load;

M_{ASCE} = flexural strength calculated using ASCE specification;

M_b = flexural strength about the centroidal axis;

M_{DSM} = flexural strength calculated using direct strength method;

M_e = second-order elastic moment;

M_{end} = end moment;

$M_{end,d}$ = end moment calculated by design rules;

$M_{end,FEA}$ = end moment obtained from FEA;

$M_{end,TEST}$ = end moment obtained from tests;

$M_{end,u}$ = end moment at ultimate strength;

$M_{e,u}$ = second-order elastic moment at ultimate strength;

M_{FEA} = flexural strength obtained using FEA;

M_n = nominal flexural strength for beams;

M_{ne} = pure flexural capacity;

M_{ocr} = moment causing local buckling under combined compression and bending;

M_{one} = overall flexural capacity;

M_{TEST} = flexural strength obtained from tests;

M_u = flexural strength;

M_y = first yield moment;

r_{cr} = radial distance of local buckling load;

r_i = radius of corner of cross section;

r_{ne} = radial distance of overall capacity;

r_n = radial distance of strength;

S_y = elastic section modulus;

t = plate thickness of specimen;

λ_c = column slenderness;

λ_n = beam-column slenderness;

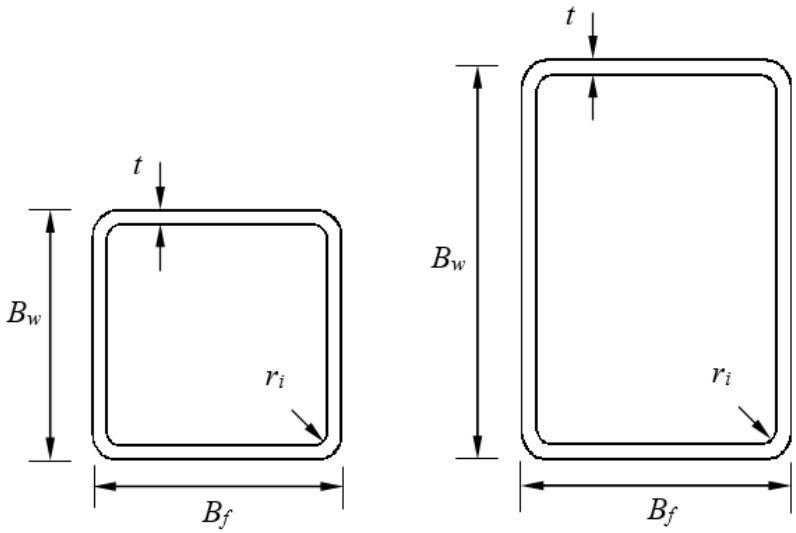

Fig. 1 Definition of symbols

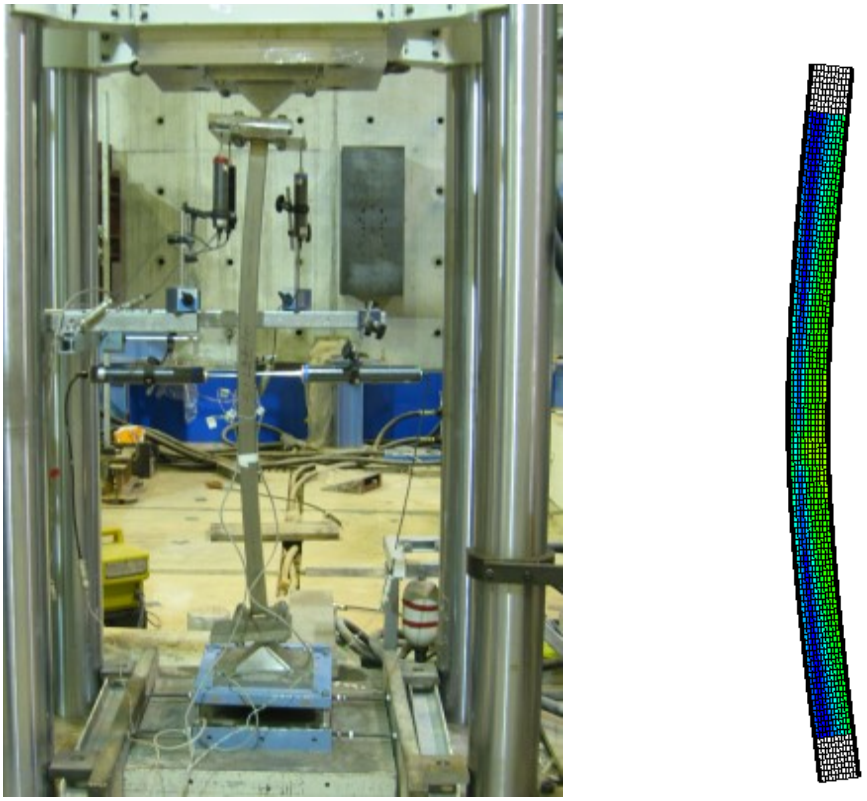

Fig. 2 Comparison of experimental [22] and FEA deformed shape for specimen S1L2E10

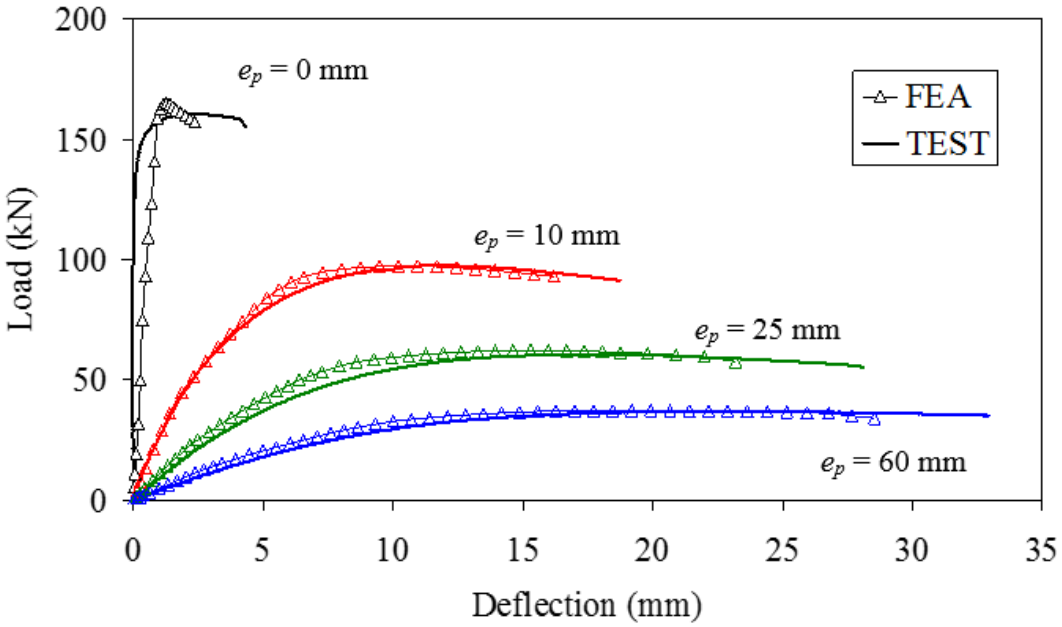

Fig. 3 Load-deflection curves for Series S1L1

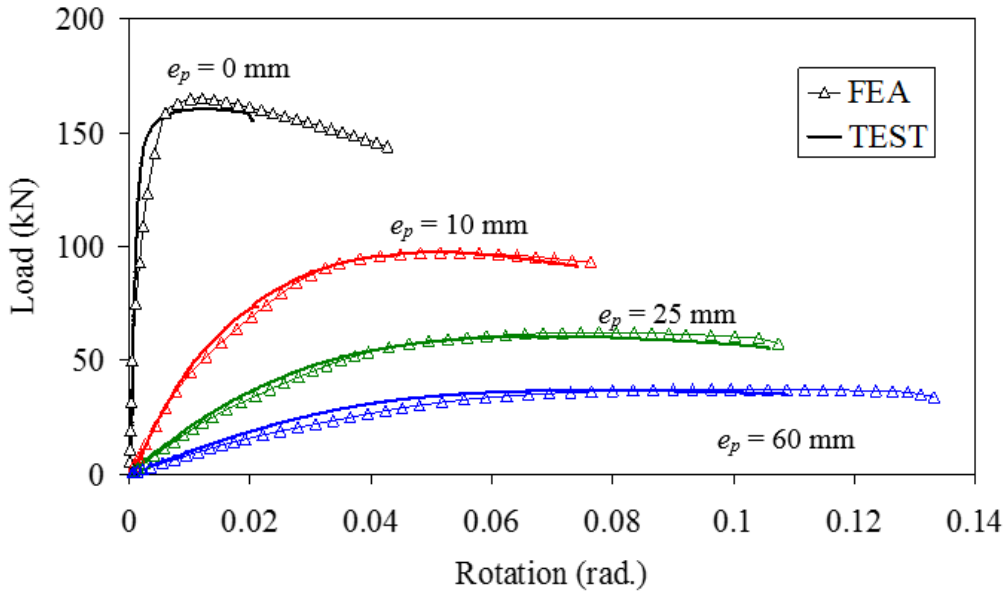

Fig. 4 Load-rotation curves for Series S1L1

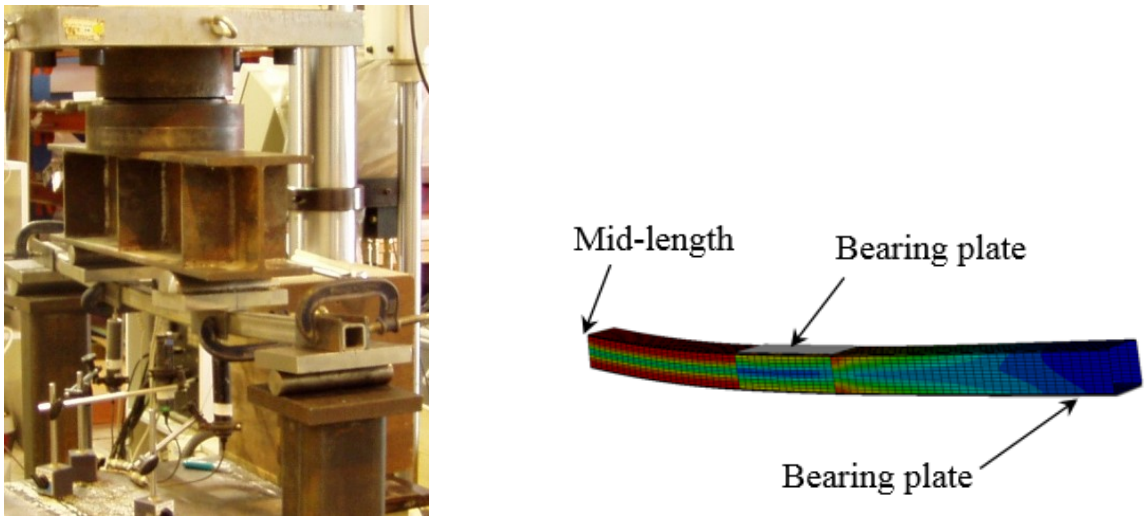

Fig. 5 Comparison of experimental specimen [12] and FEA model for beam specimen N40×40×2

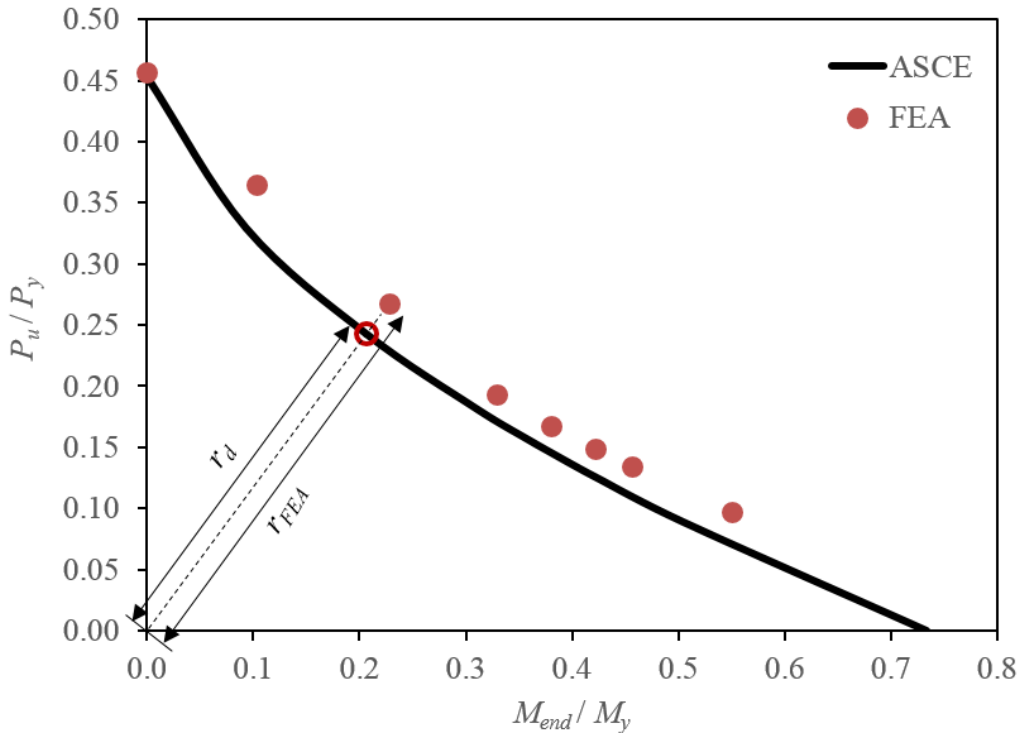

Fig. 6 Direct comparison between FEA predictions and design predictions in normalized load-moment diagram

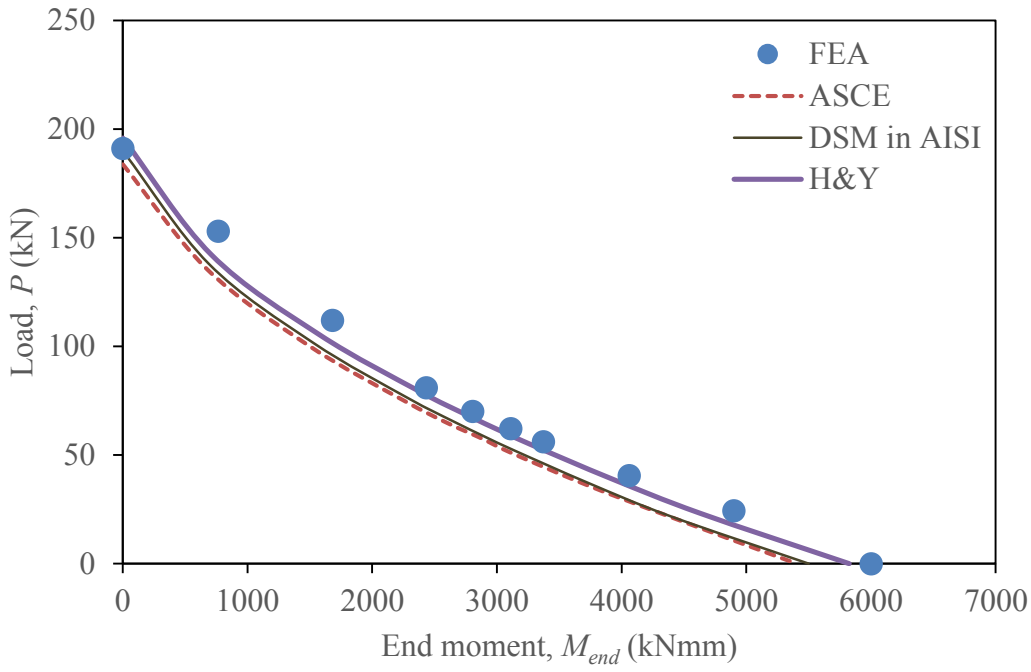

(a) Load and end moment relationship

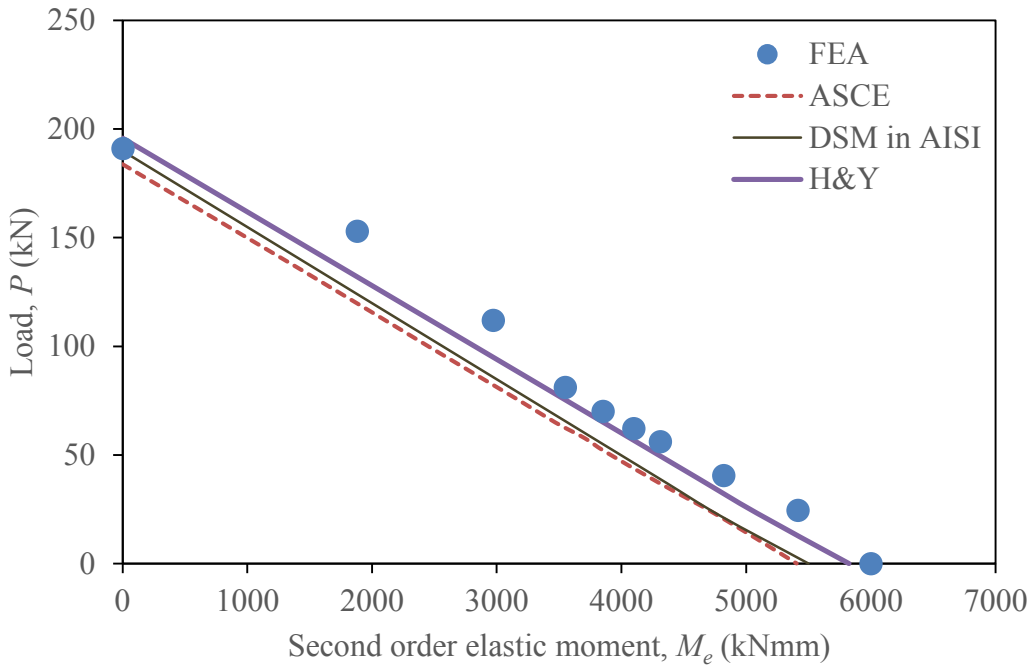

(b) Load and second order elastic moment relationship

Fig. 7 Comparison of FEA results with design strengths calculated by linear interaction load-moment curve for Series HS100-50-1400

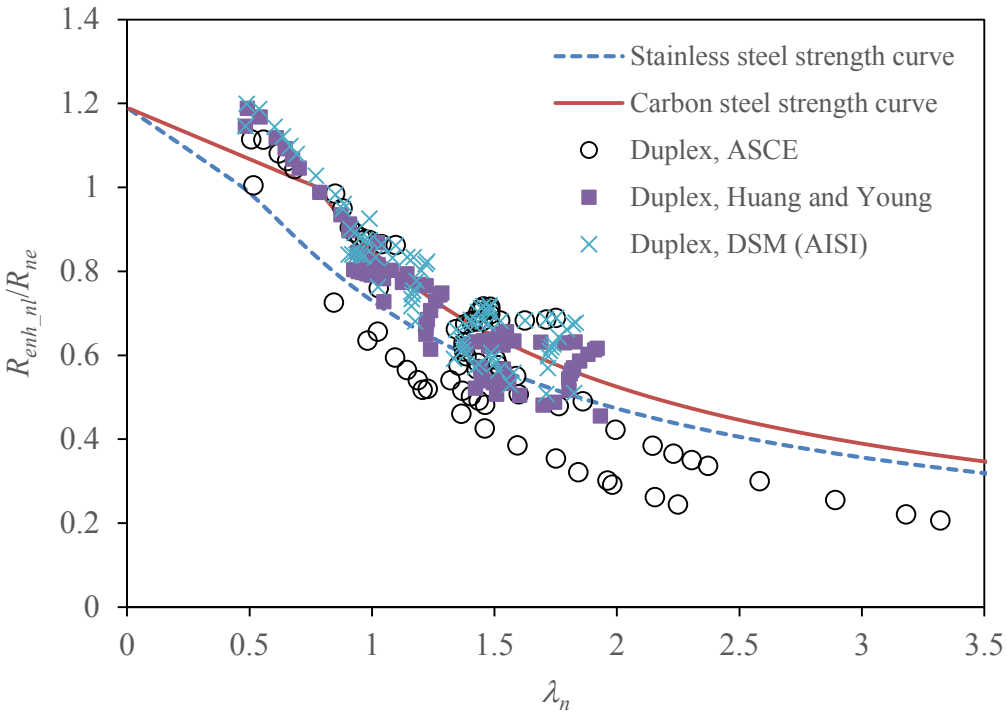

Fig. 8 Comparison of FEA results with direct strength method for duplex stainless steel beam-columns proposed by Arrayago et al. [27]

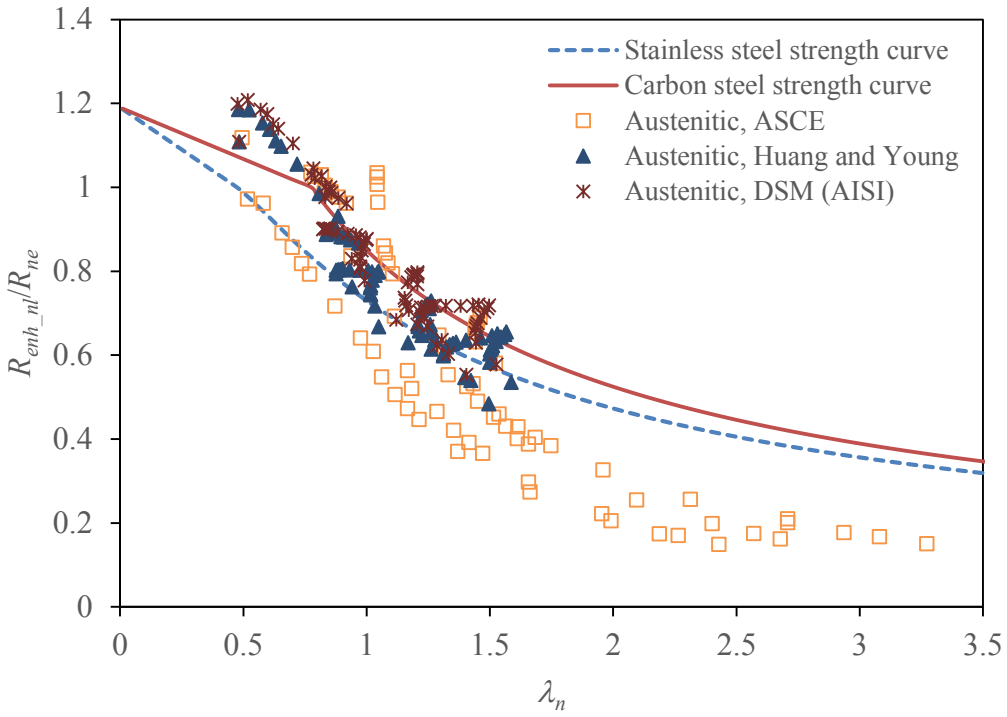

Fig. 9 Comparison of FEA results with direct strength method for austenitic stainless steel beam-columns proposed by Arrayago et al. [27]

Specimen	Dimension (mm)					
	B_w	B_f	t	r_i	L	l_e
S1L1	40.2	39.9	1.919	2.3	550	630
S1L2	40.2	40.0	1.954	2.3	1100	1180
S2L1	50.2	50.1	1.538	2.3	550	630
S2L2	50.1	50.0	1.534	2.3	1100	1180

Table 1: Mean value of stainless steel beam-column specimen dimensions (Lui et al. [22])

Series	Flat portion					Corner portion		
	E (GPa)	$f_{0.2}$ (MPa)	f_u (MPa)	n	m	E (GPa)	$f_{0.2}$ (MPa)	f_u (MPa)
S1	216	707	827	4.0	4.0	214	880	1170
S2	200	622	770	5.0	3.8	214	774	1029

Table 2: Material properties of stainless steel specimens (Young and Lui [48])

Specimen	Test			FEA			Comparison
	Failure mode	N_{TEST} (kN)	$M_{end-TEST}$ (kNm)	Failure mode	N_{FEA} (kN)	$M_{end-FEA}$ (kNm)	$\frac{N_{TEST}}{N_{FEA}}, \frac{M_{end-TEST}}{M_{end-FEA}}$
S1L1E00	F	160.6	0.00	F	165.1	0.00	0.97
S1L1E10	F	97.5	0.98	F	97.3	0.97	1.00
S1L1E25	F	60.6	1.52	F	62.2	1.56	0.97
S1L1E60	F	36.9	2.21	F	37.3	2.24	0.99
S1L2E00	F	76.8	0.00	F	77.8	0.00	0.99
S1L2E10	F	56.9	0.57	F	55.8	0.56	1.02
S1L2E25	F	39.5	0.99	F	40.7	1.02	0.97
S1L2E60	F	25.6	1.54	F	26.4	1.58	0.97
S2L1E00	L+F	157.6	0.00	L+F	166.3	0.00	0.95
S2L1E10	L+F	104.8	1.05	L+F	100.9	1.01	1.04
S2L1E25	L+F	66.9	1.67	L+F	67.6	1.69	0.99
S2L1E60	L+F	40.6	2.44	L+F	38.7	2.32	1.05
S2L2E10	F	70.7	0.71	F	70.3	0.71	1.01
S2L2E25	F	50.0	1.25	F	52.5	1.31	0.95
S2L2E60	L+F	31.2	1.87	F	32.9	1.97	0.95
						Mean	0.99
						COV	0.031

Table 3: Comparison of FEA results with beam-column test results obtained by Lui et al. [22]

Specimen	Dimension					Material properties			Test
	B_w (mm)	B_f (mm)	t (mm)	r_i (mm)	L (mm)	E (GPa)	$f_{0.2}$ (MPa)	f_u (MPa)	M_{TEST} (kNm)
N40×40×2	40.1	40.1	1.957	2.0	1442	194	447	704	2.35
N40×40×4	40.1	40.0	3.883	4.0	1441	196	565	725	5.11
N80×80×2	80.4	80.5	1.908	4.0	1442	201	398	608	6.64
N80×80×5	79.8	79.9	4.772	7.5	1443	194	448	618	24.78
N100×50×2	99.9	49.8	1.970	2.0	1440	198	320	635	8.81
N100×50×4	99.7	49.6	3.881	4.0	1439	195	378	603	21.28
N120×60×2	120.2	59.9	1.838	2.5	1442	200	361	646	10.25
N120×60×4	120.0	59.7	3.885	5.5	1442	200	392	696	34.09
H40×40×2	40.0	40.2	1.937	2.0	1243	216	707	827	3.45
H50×50×1.5	50.3	50.1	1.541	1.5	1242	200	622	770	3.48
H150×150×3	150.7	150.6	2.779	4.8	1640	189	448	699	31.68
H150×150×6	150.5	150.7	5.870	6.0	1650	194	497	761	108.60
H140×80×3	140.3	80.5	3.094	6.5	1440	212	486	736	33.97
H160×80×3	160.6	80.9	2.901	6.0	1440	208	536	766	39.36
H200×110×4	197.7	109.1	3.998	8.5	1644	200	503	961	80.15

Table 4: Dimension of stainless steel beam specimens and test results (Zhou and Young [12])

Specimen	M_{TEST} (kNm)	M_{FEA} (kNm)		M_{TEST} / M_{FEA}
N40×40×2	2.35	2.42		0.97
N40×40×4	5.11	5.37		0.95
N80×80×2	6.64	6.94		0.96
N80×80×5	24.78	24.89		1.00
N100×50×2	8.81	9.19		0.96
N100×50×4	21.28	22.73		0.94
N120×60×2	10.25	11.03		0.93
N120×60×4	34.09	33.63		1.01
H40×40×2	3.45	3.45		1.00
H50×50×1.5	3.48	3.62		0.96
H150×150×3	31.68	32.85		0.96
H150×150×6	108.60	111.38		0.98
H140×80×3	33.97	35.80		0.95
H160×80×3	39.36	41.07		0.96
H200×110×4	80.15	80.20		1.00
			Mean	0.97
			COV	0.025

Table 5: Comparison of FEA results with beam test results obtained by Zhou and Young [12]

Specimen	Dimension					
	B_w (mm)	B_f (mm)	t (mm)	r_i (mm)	L (mm)	l_e (mm)
100-50-1400	50	100	2.0	2.3	1400	1480
100-50-2800	50	100	2.0	2.3	2800	2880
150-100-1400	100	150	2.0	2.3	1400	1480
150-100-2800	100	150	2.0	2.3	2800	2880
100-100-1400	100	100	2.0	2.3	1400	1480
100-100-2800	100	100	2.0	2.3	2800	2880
180-180-1400	180	180	3.0	5.3	1400	1480
180-180-2800	180	180	3.0	5.3	2800	2880

Table 6: Dimension of stainless steel SHS and RHS specimens in parametric study

Material	E (GPa)	$f_{0.2}$ (MPa)	f_u (MPa)	ε_u (%)	n	m
Duplex (HS)	227	731	870	15.8	4.8	3.9
Austenitic (NS)	187	398	709	60.6	6.4	3.0

Table 7: Material properties of specimens used in parametric study

		Linear interaction			Direct strength method in Arrayago et al. [27]					
		$\frac{r_{FEA}}{r_{ASCE}}$	$\frac{r_{FEA}}{r_{DSM}}$	$\frac{r_{FEA}}{r_{H\&Y}}$	$\frac{r_{FEA}}{r^*_{CS,ASCE}}$	$\frac{r_{FEA}}{r^*_{CS,DSM}}$	$\frac{r_{FEA}}{r^*_{CS,H\&Y}}$	$\frac{r_{FEA}}{r^*_{SS,ASCE}}$	$\frac{r_{FEA}}{r^*_{SS,DSM}}$	$\frac{r_{FEA}}{r^*_{SS,H\&Y}}$
HS	# of tests	79	79	79	79	79	79	79	79	79
	Mean (P_m)	0.99	1.06	1.01	0.87	1.01	0.97	0.98	1.16	1.10
	COV(V_P)	0.106	0.093	0.099	0.201	0.088	0.091	0.207	0.085	0.089
	Reliability index (β)	2.56	2.88	2.68	1.71	2.72	2.52	2.08	3.25	3.03
NS	# of tests	79	79	79	79	79	79	79	79	79
	Mean (P_m)	0.98	1.04	0.98	0.76	0.99	0.93	0.88	1.15	1.08
	COV(V_P)	0.110	0.088	0.100	0.318	0.064	0.066	0.334	0.069	0.076
	Reliability index (β)	2.52	2.80	2.52	1.01	2.70	2.44	1.32	3.31	3.01
All	# of tests	158	158	158	158	158	158	158	158	158
	Mean (P_m)	0.99	1.05	0.99	0.82	1.00	0.95	0.93	1.15	1.09
	COV(V_P)	0.108	0.091	0.101	0.267	0.078	0.082	0.277	0.077	0.083
	Reliability index (β)	2.55	2.84	2.60	1.32	2.71	2.47	1.66	3.28	3.02

Note: Resistance factor = 0.85; *Direct strength method in Arrayago et al. [27] is used to consider local buckling and strength enhancement.

Table 8: Comparison of FEA results with design strengths of beam-column members

		$\frac{P_{FEA}}{P_{ASCE}}$	$\frac{P_{FEA}}{P_{DSM}}$	$\frac{P_{FEA}}{P_{H\&Y}}$	$\frac{M_{FEA}}{M_{ASCE}}$	$\frac{M_{FEA}}{M_{DSM}}$	$\frac{M_{FEA}}{M_{H\&Y}}$
HS	# of tests	8	8	8	4	4	4
	Mean (P_m)	0.88	1.07	1.02	1.10	1.18	1.11
	COV(V_P)	0.113	0.065	0.074	0.057	0.070	0.067
NS	# of tests	8	8	8	4	4	4
	Mean (P_m)	0.81	1.07	0.98	1.13	1.13	1.06
	COV(V_P)	0.098	0.065	0.092	0.055	0.045	0.047
All	# of tests	16	16	16	8	8	8
	Mean (P_m)	0.85	1.06	1.00	1.11	1.15	1.08
	COV(V_P)	0.098	0.073	0.085	0.055	0.060	0.061

Table 9: Comparison of FEA results with design strengths of column members and beam members